JACS
JOURNAL OF THE AMERICAN CHEMICAL SOCIETY
Article
pubs.acs.org/JACS

Template-Directed Synthesis of Nets Based upon Octahemioctahedral Cages That Encapsulate Catalytically Active Metalloporphyrins

Zhenjie Zhang,[†] Linping Zhang,[†] Lukasz Wojtas,[†] Mohamed Eddaoudi,[†,‡] and Michael J. Zaworotko*[,†]

[†]Department of Chemistry, University of South Florida, 4202 East Fowler Avenue, CHE205, Tampa, Florida 33620, United States
[‡]Chemical Science, 4700 King Abdullah University of Science and Technology, Thuwal 23955-6900, Kingdom of Saudi Arabia

Supporting Information

ABSTRACT: *meso*-Tetra(*N*-methyl-4-pyridyl)porphine tetratosylate (TMPyP) templates the synthesis of six new metal−organic materials by the reaction of benzene-1,3,5-tricarboxylate with transition metals, five of which exhibit HKUST-1 or **tbo** topology (M = Fe, Mn, Co, Ni, Mg). The resulting materials, **porph@MOMs**, selectively encapsulate the corresponding metalloporphyrins in octahemioctahedral cages and can serve as size-selective heterogeneous catalysts for oxidation of olefins.

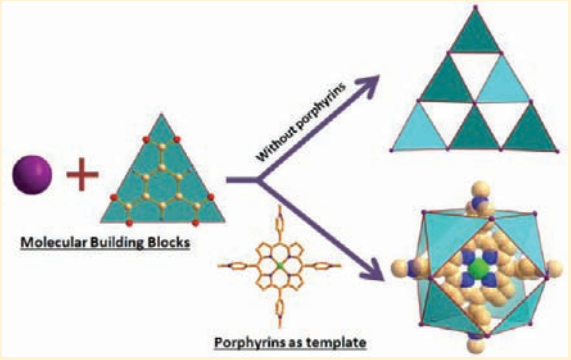

INTRODUCTION

Metal−organic materials (MOMs) are composed of metals or metal clusters ("nodes") coordinated to multifunctional organic ligands ("linkers"),[1,2] and they can offer unparalleled levels of permanent porosity. Indeed, there are numerous MOMs with Brunauer−Emmett−Teller (BET) surface areas in the 3000−6000 m^2/g range.[3] Furthermore, the modular nature of MOMs and their use of known coordination chemistry afford enormous diversity of structures[4] and properties.[5−7] The versatility of MOMs is exemplified by the manner in which porphyrins, which are widely used as catalysts and dyes,[8] can be incorporated into MOMs (Scheme 1): porphyrin-walled MOMs (**porphMOMs**) are generated from custom-designed porphyrins that possess coordinating moieties at their peripheries;[9−11] porphyrin-encapsulated MOMs (**porph@MOMs**) are prepared from MOMs that contain polyhedral cages with the requisite size and shape. Robson,[12] Goldberg,[13] and Suslick[14] pioneered **porphMOMs**, and they continue to attract attention for their utility in gas storage and/or catalysis.[15−19] MOMs based upon multiple polyhedral cages[20,21] offer excellent platforms for the development of heterogeneous catalytic systems, since in principle, cages with the requisite symmetry and size to accommodate a catalytic metalloporphyrin in a "ship-in-a-bottle" fashion can be connected to pores that facilitate ingress of substrate and egress of product. However, porphyrin encapsulation has been reported in only three structurally characterized MOMs: a discrete pillared coordination box (**porph@MOM-1**),[22] a zeolitic metal−organic framework (MOF) that exhibits **rho**-zeolite topology (**porph@MOM-2**),[23] and the prototypal polyhedral MOM, HKUST-1 (**porph@MOM-3**).[24] HKUST-1 is formed via assembly of benzene-1,3,5-tricarboxylate (BTC) anions and Cu^{2+} (HKUST-1-Cu),[21] Zn^{2+} (HKUST-1-Zn),[25] Fe^{2+}/Fe^{3+} (HKUST-1-Fe),[26] or Ni^{2+} (HKUST-1-Ni)[27] cations and is well-suited to serve as a platform for catalysis since its topology affords three distinct polyhedral cages. Indeed, HKUST-1-Cu selectively encapsulates polyoxometalate anions in its octahemioctahedral cages and exhibits size-selective catalysis of ester hydrolysis.[28] However, the **tbo** topology of HKUST-1 requires "square paddlewheel" nodes that are not readily accessible for metals other than Cu^{2+} and Zn^{2+}.

Scheme 1. Illustration of PorphMOMs and Porph@MOMs

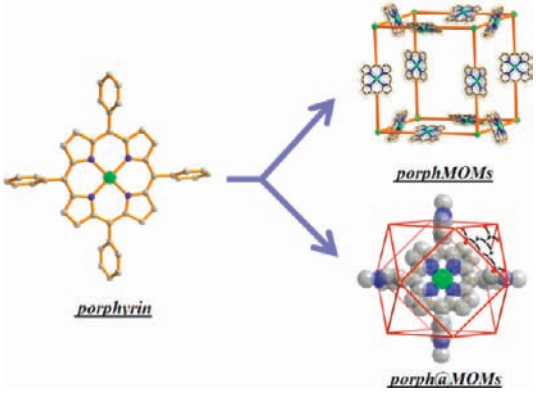

Received: September 1, 2011
Published: December 13, 2011

dx.doi.org/10.1021/ja208256u | J. Am. Chem.Soc. 2012, 134, 928−933

In this contribution, we address the dearth of **porph@MOMs** by exploring whether porphyrins can serve as templates for their generation. Template-directed synthesis has been widely explored in the context of zeolites[29] but remains underexplored in the context of MOMs. Two recent examples include a study by Bajpe et al.[30] on the templating effect of Keggin ions upon the formation of HKUST-1-Cu and a study by Bannerjee and co-workers[31] on template-induced structural isomerism. The latter studies inspired us to investigate how *meso*-tetra(*N*-methyl-4-pyridyl)porphine tetratosylate (TMPyP), a widely studied catalyst,[32] might serve as a template for the formation of octahemioctahedral cages and thereby generate new variants of HKUST-1. We present herein the solvothermal synthesis, structural characterization, and catalytic properties of six such **porph@MOMs**: $[Fe_{12}(BTC)_8(S)_{12}]$-$Cl_6 \cdot x$FeTMPyPCl$_5$ (**porph@MOM-4**), $[Co_{12}(BTC)_8(S)_{12}]\cdot x$CoTMPyPCl$_4$ (**porph@MOM-5**), $[Mn_{12}(BTC)_8(S)_{12}]\cdot x$MnTMPyPCl$_5$ (**porph@MOM-6**), $[Ni_{10}(BTC)_8(S)_{24}]\cdot x$NiTMPyP$\cdot(H_3O)_{(4-4x)}$ (**porph@MOM-7**), $[Mg_{10}(BTC)_8(S)_{24}]\cdot x$MgTMPyP$\cdot(H_3O)_{(4-4x)}$ (**porph@MOM-8**), and $[Zn_{18}(OH)_4(BTC)_{12}(S)_{15}]\cdot x$ZnTMPyP$\cdot(H_3O)_{(4-4x)}$ (**porph@MOM-9**), where x is the percent loading of porphyrin and S represents the solvent. The crystal structures revealed that metalloporphyrins are indeed selectively trapped within octahemioctahedral cages.

EXPERIMENTAL SECTION

General Information. All reagents were purchased from Fisher Scientific or Frontier Scientific and used without further purification. Solvents were purified according to standard methods and stored in the presence of molecular sieves. Thermogravimetric analysis (TGA) was performed under nitrogen on a TA Instrument TGA 2950 Hi-Res. Powder X-ray diffraction (PXRD) data were recorded on a Bruker D8 Advance X-ray diffractometer operated at 20 kV and 5 mA using Cu Kα radiation (λ = 1.5418 Å) with a scan speed of 0.5 s/step (6°/min) and a step size of 0.05°. Calculated PXRD patterns were generated using Powder Cell for Windows version 2.4 (Kraus and G. Nolze, BAM Berlin, 2000). UV spectra were measured on a PerkinElmer Lambda 35 UV−Vis−NIR spectrometer. GC−MS data were obtained on an HP 6890 series GC system equipped with a 5971A mass-selective detector. Surface areas were measured on an ASAP 2020 surface area and pore size analyzer and a QUADRASORB Sl four-station surface area and pore size analyzer.

Synthesis of ***Porph@MOM-4***. $FeCl_2\cdot 4H_2O$ (238.8 mg, 1.20 mmol), BTC (126.0 mg, 0.60 mmol), and TMPyP (8.4 mg, 0.0063 mmol) were added to a 19.5 mL solution of *N*,*N*-dimethylformamide (DMF) (16.5 mL) and H_2O (3.0 mL) in a 20 mL scintillation vial. The reaction mixture was heated to 85 °C for 12 h. Dark-red cubic crystals of **porph@MOM-4** were harvested and washed with methanol (yield: 20% based on $FeCl_2\cdot 4H_2O$).

Synthesis of ***Porph@MOM-5***. $CoCl_2\cdot 4H_2O$ (47.6 mg, 0.20 mmol), BTC (21.0 mg, 0.10 mmol), and TMPyP (2.8 mg, 0.0021 mmol) were added to a 3.5 mL solution of DMF (3.0 mL) and H_2O (0.5 mL) in a 7 mL scintillation vial. The reaction mixture was heated to 85 °C for 12 h. Dark-red cubic crystals of **porph@MOM-5** were harvested and washed with methanol (yield: 15% based on $CoCl_2\cdot 4H_2O$).

Synthesis of ***Porph@MOM-6***. A similar procedure as for **porph@MOM-5** was used, with $CoCl_2\cdot 4H_2O$ replaced by $MnCl_2\cdot 4H_2O$ (38.4 mg, 0.20 mmol). Dark-red cubic crystals of **porph@MOM-6** were harvested and washed with methanol (yield: 6% based on $MnCl_2\cdot 4H_2O$).

Synthesis of ***Porph@MOM-7***. $Ni(OAc)_2\cdot 4H_2O$ (8.3 mg, 0.03 mmol), BTC (10.5 mg, 0.05 mmol), and TMPyP (2.0 mg, 0.0015 mmol) were added to a 2.4 mL solution of DMF (2.0 mL) and H_2O (0.4 mL) in a 7 mL scintillation vial. The reaction mixture was heated to 85 °C for 48 h. Red octahedral crystals of **porph@MOM-7** were harvested and washed with methanol [yield: 66% based on $Ni(OAc)_2\cdot 4H_2O$].

Synthesis of ***Porph@MOM-8***. $Mg(OAc)_2\cdot 4H_2O$ (6.4 mg, 0.03 mmol), BTC (10.5 mg, 0.05 mmol), and TMPyP (2.0 mg, 0.0015 mmol) were added to a 2.4 mL solution of DMF (2.0 mL) and H_2O (0.4 mL). The mixture was sealed in a Pyrex tube under vacuum and heated to 85 °C for 12 h. Black cubic crystals of **porph@MOM-8** were harvested and washed with methanol [yield: 31% based on $Mg(OAc)_2\cdot 4H_2O$].

Synthesis of ***Porph@MOM-9***. $Zn(NO_3)_2\cdot 6H_2O$ (59.5 mg, 0.20 mmol), BTC (21.0 mg, 0.10 mmol), and TMPyP (2.8 mg, 0.0021 mmol) were added to a 3.5 mL solution of *N*,*N*-dimethylacetamide (DMA) (3.0 mL) and H_2O (0.5 mL) in a 7 mL scintillation vial. The reaction mixture was heated to 85 °C for 24 h. Black block crystals of **porph@MOM-9** were harvested and washed with methanol [yield: 62% based on $Zn(NO_3)_2\cdot 6H_2O$].

Single-Crystal X-ray Diffraction. Data for crystals of **porph@MOM-5**, **-6**, and **-9** were collected at the Advanced Photon Source on beamline 15ID-C of ChemMatCARS Sector 15 [λ = 0.40663 Å, T = 100(2) K]. The data for the remaining **porph@MOMs** were collected on a Bruker AXS SMART APEX/CCD diffractometer using Cu Kα radiation [λ = 1.5418 Å, T = 100(2) K]. Indexing was performed using APEX2 (difference vectors method). Data integration and reduction were performed using SAINT-Plus 6.01. Scaling and absorption correction were performed by a multiscan method implemented in SADABS.[33] Space groups were determined using XPREP as implemented in APEX2. The structures were solved using SHELXS-97 (direct methods) and refined using SHELXL-97 (full-matrix least-squares on F^2) as contained in the APEX2 and WinGX v1.70.01 program packages.[34] For all structures, the metal atoms of the porphyrin core were located via difference Fourier map inspection and refined anisotropically. Site occupancy was determined through refinement. In **porph@MOM-7** and **-9**, the contribution of disordered porphyrin organic parts and solvent molecules was treated as diffuse using the SQUEEZE procedure implemented in PLATON,[35] whereas for **porph@MOM-4**, **-5**, and **-6**, non-hydrogen atoms of the porphyrins were refined isotropically using geometry restraints. For the coordinated solvents, only O atoms were refined. The contribution of disordered solvent molecules and cations was treated as diffuse using the SQUEEZE procedure implemented in PLATON.

Procedure for Catalysis Reactions. Crystals of **porph@MOM-4** (10.0 mg) were immersed in acetonitrile for 48 h, filtered, and placed in a solution of olefin (1.0 mmol), aqueous *tert*-butyl hydroperoxide (t-BuOOH) (195.0 μL, 1.5 mmol), 1,2-dichlorobenzene (internal standard, 50.0 μL), and acetonitrile (5.0 mL). The reaction mixture was heated at 60 °C for 10 h and monitored by GC−MS (HP-5MS column, 5% phenyl methyl siloxane, 30 m × 0.25 mm × 0.25 μm; injector temperature 250 °C). Method for styrene: hold for 1 min at 50 °C, then rise to 120 °C at 7 °C/min; detector temperature, 170 °C; carrier gas, He (1.1 mL/min). Styrene, 4.7 min; benzaldehyde, 6.1 min; 1,2-dichlorobenzene, 7.5 min; styrene oxide, 8.2 min; benzoic acid, 11.8 min. Method for *trans*-stilbene: hold for 1 min at 100 °C, then rise from 100 to 180 °C at 2 °C/min, and finally hold at 180 °C for 3 min; detector temperature, 170 °C; carrier gas, He (1.1 mL/min). Benzaldehyde, 2.52 min; 1,2-dichlorobenzene, 6.5 min; benzoic acid, 7.1 min; stilbene, 27.1 min; stilbene oxide, 27.6 min. Method for triphenylethylene: hold for 1 min at 50 °C, rise to 160 °C at 10 °C/min, then rise from 160 to 200 °C with 2 °C/min, and finally hold for 1 min at 200 °C; detector, 170 °C; carrier gas, He (1.1 mL/min). Benzaldehyde, 5.7 min; 1,2-dichlorobenzene, 6.5 min; benzoic acid, 7.6 min; benzoic acid butyl ester, 9.6 min; diphenylmethanone, 15.6 min; triphenylethylene, 33.7 min. After the catalytic reaction, the reaction solution was filtered and the filtrant recycled. Reaction with an equivalent molar amount of commercial FeTMPyP and a control reaction without catalyst were conducted under the same conditions.

RESULTS AND DISCUSSION

Structural Description of Porph@MOM-4, -5, and -6. The reaction of M(II)Cl_2 (M = Fe, Co, Mn) with BTC and

dx.doi.org/10.1021/ja208256u | J. Am. Chem.Soc. 2012, 134, 928−933

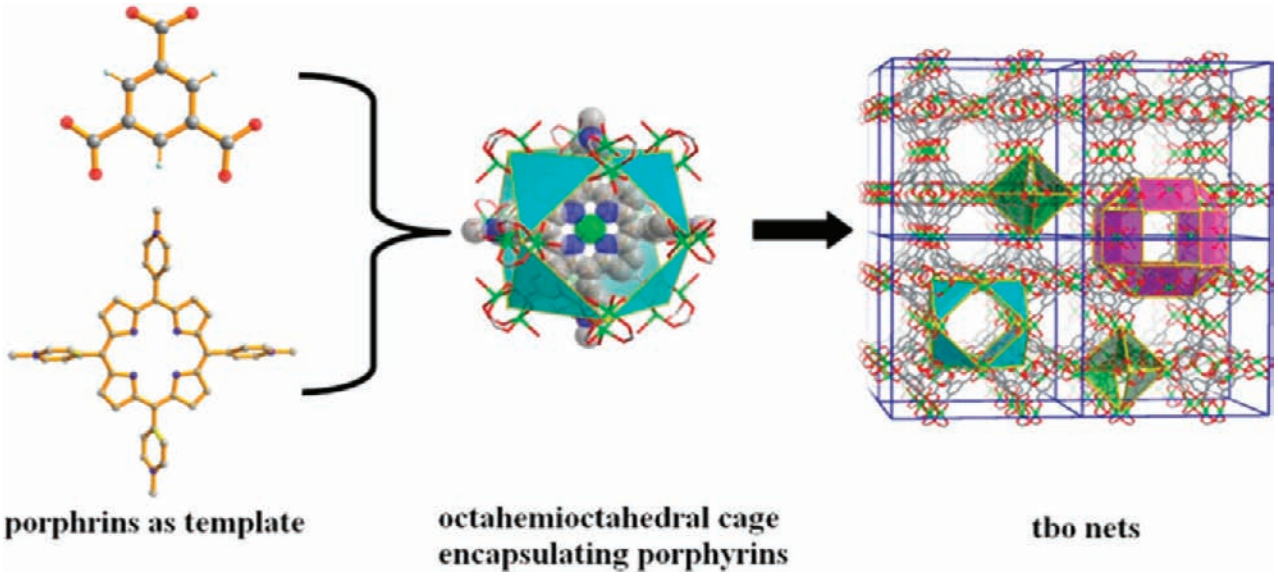

Figure 1. (right) Polyhedral cage framework of **porph@MOM-4**, **-5**, and **-6** containing three distinct cages: large rhombihexahedral cages (pink), medium-sized octahemioctahedral cages (turquoise), and small tetrahedral cages (green). (middle) TMPyP cation encapsulated in the octahemioctahedral cage. (left) Structures of BTC and TMPyP.

TMPyP in DMF and H_2O afforded dark-red cubic crystals of **porph@MOM-4**, **-5**, and **-6** that adopt space group $Fm\bar{3}m$ with a = 26.597(2), 26.572(2), and 26.429(1) Å, respectively. All three compounds are isostructural with HKUST-1 and therefore exhibit the twisted boracite (**tbo**) topology based upon 3-connected BTC ligands and 4-connected $[M_2(COO)_4]$ square paddlewheels. The **tbo** structure can be interpreted from two viewpoints, the "polyhedral" approach and the "net" approach. In the polyhedral approach, the entire framework can be disassembled into three polyhedral cages with 1:1:2 stoichiometry (Figure 1): rhombihexahedral, octahemioctahedral, and tetrahedral, respectively. The octahemioctahedral cage is the only cage that is suited for encapsulation of tetrasubstituted porphyrin molecules, since its O_h symmetry matches the porphyrin's D_{4h} symmetry (as a subgroup) and the spherical cavity (diameter ~13 Å) is a good size fit for the porphyrin ring of TMPyP (diameter ~10 Å). Moreover, the four *N*-methyl-4-pyridyl groups in TMPyP can extend through four of the six square windows of the cage (~9 Å × 9 Å, measured from the center of one paddlewheel to the adjacent paddlewheel). The TMPyP molecules are disordered over three positions [Figure S1 in the Supporting Information (SI)]. The rhombihexahedral or nanoball[36,37] cage also possesses O_h symmetry, and its internal diameter is ~15 Å. However, the internal volume is reduced by axially coordinated solvent molecules. There are no such issues with the octahemioctahedral cage because the coordinated solvent molecules are oriented toward the exterior of the cavity (Figure S1). The tetrahedral cage possesses T_d symmetry, which cannot be matched to the symmetry of the porphyrin, and its internal cavity (~6 Å diameter) is too small to accommodate porphyrins. The HKUST-1 framework can also be interpreted using the net approach. The BTC ligand contains 1,3-benzendicarboxylate (1,3-BDC) moieties in which each carboxylate group bends at ~4° with respect to the plane of benzene ring. This enables the BDC moieties to form four kinds of nanoscale secondary building units (nSBUs):[38] triangle, hexagon, 1,3-alternate-square, and cone-square (Figure S2). These nSBUs can further self-assemble into discrete polyhedral or infinite networks: triangle nSBUs together with cone-square nSBUs form nanoballs (i.e., the rhombihexahedron cages); triangle nSBUs together with hexagon nSBUs form a 2D kagomé net; 1,3-alternate-square nSBUs and cone-square nSBUs form an undulating square grid. All of these structures are known to exist when 1,3-BDC links square-paddlewheel moieties.[39] Figure 2 shows how square paddlewheels can serve as pillars to link the 2D square grid or kagomé nets into 3D networks. Figure 2 also reveals how TMPyP molecules lie in the interlayer region in a sandwich fashion. Moreover, as shown in Figure 3, the FO electron density map clearly indicates how

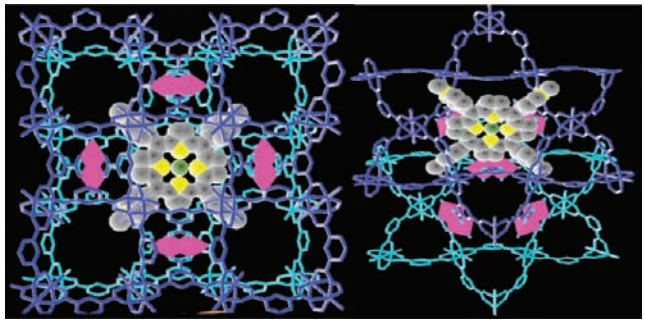

Figure 2. The two pillared-layer linking modes in **porph@MOM-4**, **-5** and **-6**: (left) pillared grid; (right) pillared kagomé. Paddlewheels serve as pillars and are illustrated in pink polyhedral mode.

the porphyrin moieties are located within the octahemioctahedral cages of **porph@MOM-4**, **-5**, and **-6**.[40]

Structural Description of Porph@MOM-7 and -8. The reaction of $Ni(OAc)_2$ with BTC and TMPyP under conditions similar to those used for **porph@MOM-5** afforded red octahedral crystals of a new variant of HKUST-1. **Porph@MOM-7** exhibits a structure having the same space group and **tbo** topology as HKUST-1-Ni. but its unit cell parameter a = 27.478(2) Å (Figure S3) is larger than that of HKUST-1-Ni [26.5941(7) Å]. The reason for the difference is that whereas HKUST-1-Ni[27] was formed from square paddlewheels, the 4-

dx.doi.org/10.1021/ja208256u | *J. Am. Chem.Soc.* 2012, 134, 928–933

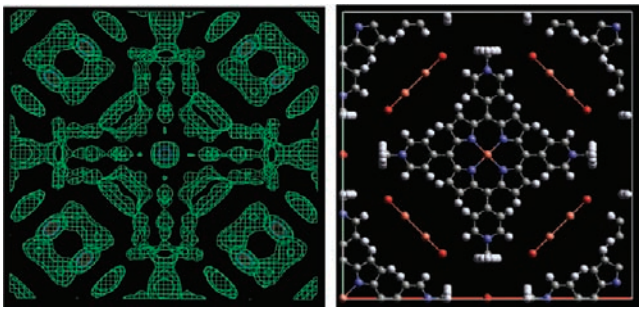

Figure 3. (left) FO electron density map indicating the position of the porphyrin moieties in **porph@MOM-4**, **-5** and **-6**. (right) Model of the location of porphyrin moieties. The map was plotted using MCE version 2005 2.20 at 0.46 el/A3 level.[40]

connected molecular building blocks in **porph@MOM-7** are modeled to be a combination of dimetallic $[M_2(\mu_2\text{-}H_2O)(COO)_4]$ and monometallic $[M(COO)_4]^{2-}$ 4-connected nodes with 1:2 stoichiometry (Figure 4 and Figure S4). Data refinement and electron density maps (Figure S5) confirmed that the metalloporphyrin moieties are located within the octahemioctahedral cages, as expected. Reaction of $Mg(OAc)_2$ with BTC and TMPyP in sealed Pyrex tubes afforded **porph@MOM-8**, a compound with a PXRD diffractogram closely matching that of **porph@MOM-7** (Figure S6).

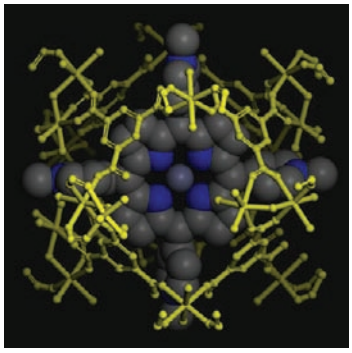

Figure 4. Simulated porphyrin cation in the octahemioctahedral cage in **porph@MOM-7**.

Structural Description of Porph@MOM-9. The reaction of $Zn(NO_3)_2$ with BTC and TMPyP in DMA and H_2O afforded black block crystals of **porph@MOM-9** in the orthorhombic space group *Cmmm* with a = 19.653(3) Å, b = 44.127(6) Å, c = 14.543(2) Å, and V = 12612(3) Å^3. **Porph@MOM-9** also contains octahemioctahedral cages, but they are sustained by two zinc molecular building blocks (Figure 5 left): $[Zn_2(COO)_4]$ paddlewheel moieties and trimetallic $[Zn_3(\mu_3\text{-}OH)(COO)_6]^-$ clusters.[41] Linking the resulting octahemioctahedral cages with BTC ligands results in a novel 3,3,4,4,6-connected net (Figure S7) with Schläfli symbol $\{4{\cdot}6^2\}_4\{4{\cdot}8^2\}_8\{4^3{\cdot}6^4{\cdot}8^8\}_4\{6^2{\cdot}8^4\}\{8^6\}_2$. Because the trimetallic $[Zn_3(\mu_3\text{-}OH)(COO)_6]^-$ building blocks are anionic, the resulting framework is anionic. Data refinement and electron density maps (Figure 6) confirmed that cationic metalloporphyrin moieties are located within the octahemioctahedral cages in a stoichiometry that balances the charge of the anionic framework. Removal of solvent molecules would create an accessible free volume of ~6986 Å^3 (55% of the volume of the unit cell).[42]

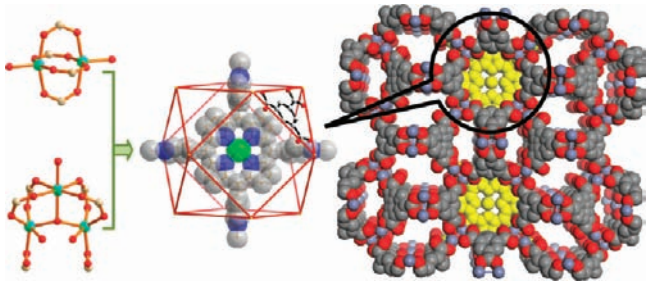

Figure 5. (left) The two molecular building blocks in **porph@MOM-9**. (middle) Porphyrin cation located in an octahemioctahedral cage. (right) Space-filling model of **porph@MOM-9** projected along the *c* axis.

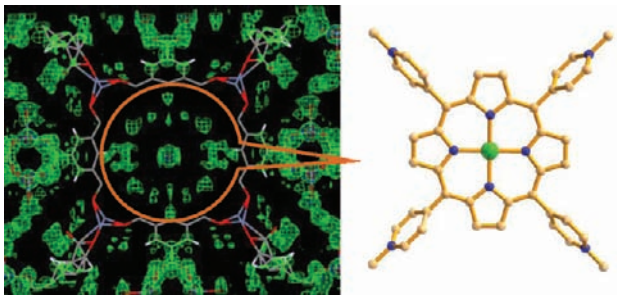

Figure 6. (left) FO electron density map indicating the possible position of the porphyrin cations in the unit cell of **porph@MOM-9** using MCE version 2005 2.20 at 1.30 el/A3 level. (right) Structure of the ZnTMPyP molecule.

UV–Vis Spectral Studies. Metalloporphyrins exhibit characteristic UV–Vis Soret bands. To verify further the presence of metalloporphyrins in **porph@MOM-4–9**, their UV–Vis spectra were collected. Samples of each **porph@MOM** were dissolved in water by adding one drop of dilute HCl and diluted to adjust the absorbance to below 1. As shown in Figure 7, **porph@MOM-4–9** exhibit prominent bands at ~400, ~438, ~464, ~426, ~429, and ~441 nm respectively, which are consistent with the reported Soret bands for the corresponding metalloporphyrins.[23,43,44]

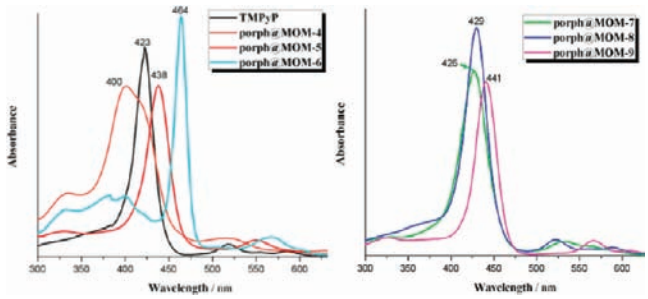

Figure 7. UV–Vis spectra of TMPyP (black), **porph@MOM-4** (orange), **porph@MOM-5** (red), **porph@MOM-6** (cyan), **porph@MOM-7** (green), **porph@MOM-8** (blue), and **porph@MOM-9** (pink) in aqueous solution.

Templating Effect and Variable Loading of TMPyP. Template-directed synthesis is a promising strategy for preparation of MOMs with structures that are otherwise hard to obtain.[45,29] **Porph@MOM-1**, **-2**, and **-3** can be generated in the absence of porphyrins; to validate the templating effect of

dx.doi.org/10.1021/ja208256u | J. Am. Chem.Soc. 2012, 134, 928–933

TMPyP in the syntheses of **porph@MOM-4−9**, we attempted these syntheses via a series of parallel experiments in which varying amounts of TMPyP were present. **Porph@MOM-4−9** could not be prepared in the absence of porphyrin. Rather, either the previously reported structures $[M_6(HCOO)(BTC)_2(DMF)_6]_n$ (M = Mn, Co)[46,47] (Figures S8 and S9) or unknown crystalline phases (Figures S6 and S10−S12) were obtained. Different proportions of TMPyP facilitated variable loading of metalloporphyrins, as exemplified by **porph@MOM-4**. Crystals of **porph@MOM-4** were prepared using different TMPyP/BTC ratios, and the porphyrin loadings were calculated using UV−Vis spectroscopy versus a reference aqueous solution of FeTMPyP. TMPyP loadings of 14−88% were observed (Figure S13).

Catalysis Study. The "ship-in-a-bottle" encapsulation of metalloporphyrins observed in **porph@MOM-4−9** prompted us to explore whether they would exhibit catalytic activity. **Porph@MOM-4** (50% loading as determined by UV−Vis spectroscopy; Langmuir surface area = 263 m^2/g; Figure 8) was selected to evaluate olefin oxidation, a classic reaction of heme enzymes.[48] As illustrated in Figure 9 and Table S1, conversion of styrene (4.2 Å × 7.0 Å cross section) reached ~85%

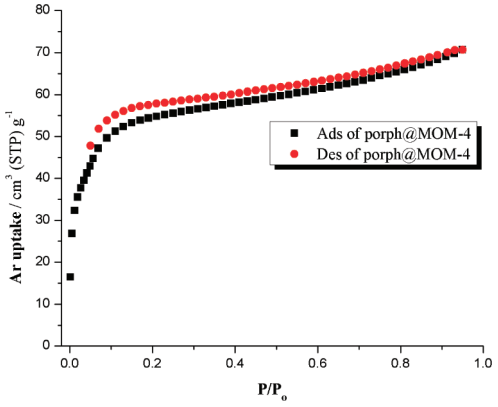

Figure 8. Ar sorption isotherm of **porph@MOM-4** at 87K.

[turnover frequency (TOF) = 269 h^{-1}] after 10 h, compared with only ~35% conversion using an equivalent amount of Fe(III)TMPyP in solution. Styrene oxide and benzaldehyde were identified as the major products (30 and 57%, respectively). This is consistent with the selectivity reported by Maurya.[49] In contrast, *trans*-stilbene (4.2 Å × 11.4 Å cross section) was only ~40% converted under the same conditions (TOF = 126 h^{-1}), compared with conversion of ~34% for FeTMPyP in solution. Stilbene oxide was the major product (70% selectivity). The conversion of triphenylethylene (9.0 Å × 11.4 Å cross section) by **porph@MOM-4** was <5% (TOF = 15 h^{-1}) under the same conditions, whereas FeTMPyP in solution exhibited ~14% conversion with diphenylmethanone and benzaldehyde being the major products. The reaction solutions were filtered after the catalytic reaction, and the filtrate showed no detectable metalloporphyrin species via UV−Vis. The filtrant was recycled, and even after seven 10 h cycles, we observed >55% conversion of styrene (Figure 10). These observations are consistent with the oxidation reaction occurring in the cages of **porph@MOM-4**, since the pores (~9 Å × 9 Å) in **porph@MOM-4** are the windows of the octahemioctahedral cages.

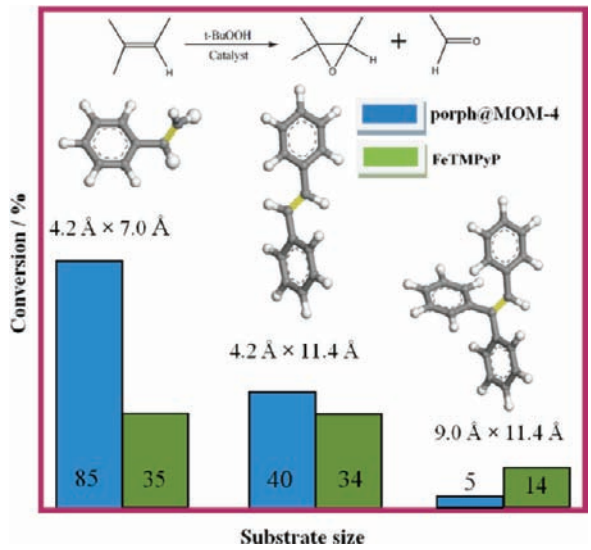

Figure 9. Catalytic effect of **porph@MOM-4** vs FeTMPyP upon substrates of different size (styrene, *trans*-stilbene, and triphenylethylene), revealing size selectivity consistent with the pore size of **porph@MOM-4**.

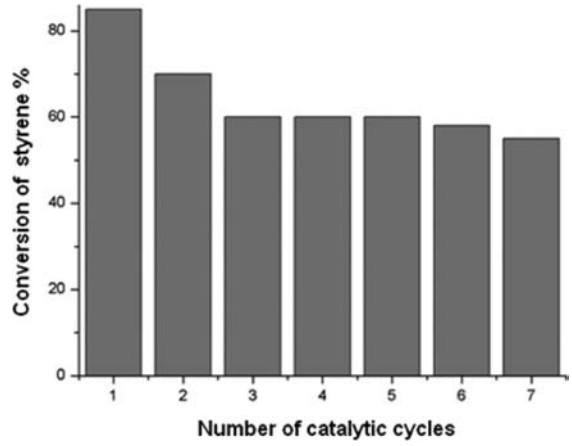

Figure 10. Catalytic activity toward styrene oxidation exhibited by recycled **porph@MOM-4** as measured by GC−MS.

CONCLUSION

We have reported herein that porphyrins template the formation of octahemioctahedral cages assembled from BTC ligands and transition metals. Five new variants of HKUST-1 nets and a new polyhedral-based net (**porph@MOM-9**) that encapsulate metalloporphyrins were thereby synthesized and characterized. Should the templating effect of porphyrins be general in nature, it would offer a new route to functional MOMs, and we are systematically exploring this possibility in our laboratories.

ASSOCIATED CONTENT

Supporting Information

Crystal data (CIF); IR, TGA, and PXRD data; structure figures; and tables and figures showing catalysis results. This material is available free of charge via the Internet at http://pubs.acs.org.

AUTHOR INFORMATION

Corresponding Author

xtal@usf.edu

■ ACKNOWLEDGMENTS

This publication is based on work supported by Award FIC/2010/06 made by King Abdullah University of Science and Technology (KAUST). The data for **porph@MOM-5**, **-6**, and **-9** were collected at the Advanced Photon Source on beamline 15ID-C of ChemMatCARS Sector 15, which is principally supported by the National Science Foundation and the Department of Energy under Grant NSF/CHE-0822838. The Advanced Photon Source is supported by the U.S. Department of Energy, Office of Science, Office of Basic Energy Sciences, under Contract DE-AC02-06CH11357.

■ REFERENCES

(1) Batten, S. R.; Neville, S. M.; Turner, D. R. *Coordination Polymers: Design, Analysis and Application*; Royal Society of Chemistry: Cambridge, U.K., 2009.
(2) *Metal−Organic Frameworks: Design and Application*; MacGillivray, L. R., Ed.; Wiley: Hoboken, NJ, 2010.
(3) Furukawa, H.; Ko, N.; Go, Y. B.; Aratani, N.; Choi, S. B.; Choi, E.; Yazaydin, A. O.; Snurr, R. Q.; O'Keeffe, M.; Kim, J.; Yaghi, O. M. *Science* **2010**, *329*, 424.
(4) Moulton, B.; Zaworotko, M. J. *Chem. Rev.* **2001**, *101*, 1629.
(5) Kitagawa, S.; Kitaura, R.; Noro, S. *Angew. Chem., Int. Ed.* **2004**, *43*, 2334.
(6) Rosseinsky, M. J. *Nat. Mater.* **2010**, *9*, 609.
(7) Seo, J. S.; Whang, D.; Lee, H.; Jun, S. I.; Oh, J.; Jeon, Y. J.; Kim, K. *Nature* **2000**, *404*, 982.
(8) Lu, H.; Zhang, X. P. *Chem. Soc. Rev.* **2011**, *40*, 1899.
(9) Suslick, K. S.; Bhyrappa, P.; Chou, J. H.; Kosal, M. E.; Nakagaki, S.; Smithenry, D. W.; Wilson, S. R. *Acc. Chem. Res.* **2005**, *38*, 283.
(10) Goldberg, I. *Chem. Commun.* **2005**, 1243.
(11) Beletskaya, I.; Tyurin, V. S.; Tsivadze, A. Y.; Guilard, R.; Stern, C. *Chem. Rev.* **2009**, *109*, 1659.
(12) Abrahams, B. F.; Hoskins, B. F.; Michail, D. M.; Robson, R. *Nature* **1994**, *369*, 727.
(13) Goldberg, I. *Angew. Chem., Int. Ed.* **1998**, *37*, 3027.
(14) Zimmerman, S. C.; Wendland, M. S.; Rakow, N. A.; Suslick, K. S. *Nat. Mater.* **2002**, *1*, 118.
(15) Choi, E.-Y.; Barron, P. M.; Novotny, R. W.; Son, H.-T.; Hu, C.; Choe, W. *Inorg. Chem.* **2009**, *48*, 426.
(16) Motoyama, S.; Makiura, R.; Sakata, O.; Kitagawa, H. *J. Am. Chem. Soc.* **2011**, *133*, 5640.
(17) Xie, M.-H.; Yang, X.-L.; Wu, C.-D. *Chem. Commun.* **2011**, *47*, 5521.
(18) Wang, X.-S.; Meng, L.; Cheng, Q.; Kim, C.; Wojtas, L.; Chrzanowski, M.; Chen, Y.-S.; Zhang, X. P.; Ma, S. *J. Am. Chem. Soc.* **2011**, *133*, 16322.
(19) Farha, O. F.; Shultz, A. M.; Sarjeant, A. A.; Nguyen, S. T.; Hupp, J. T. *J. Am. Chem. Soc.* **2011**, *133*, 5652.
(20) Perry, J. J. IV; Perman, J. A.; Zaworotko, M. J. *Chem. Soc. Rev.* **2009**, *38*, 1400.
(21) Chui, S. S.-Y.; Lo, S. M.-F.; Charmant, J. P. H.; Orpen, A. G.; Williams, I. D. *Science* **1999**, *283*, 1148.
(22) Ono, K.; Yoshizawa, M.; Kato, T.; Watanabe, K.; Fujita, M. *Angew. Chem., Int. Ed.* **2007**, *46*, 1803.
(23) Alkordi, M. H.; Liu, Y.; Larsen, R. W.; Eubank, J. F.; Eddaoudi, M. *J. Am. Chem. Soc.* **2008**, *130*, 12639.
(24) Larsen, R. W.; Wojtas, L.; Perman, J.; Musselman, R. L.; Zaworotko, M. J.; Vetromile, C. M. *J. Am. Chem. Soc.* **2011**, *133*, 10356.
(25) Lu, J.; Hajndl, R.; Hariharan, S.; Zaworotko, M. J. *Angew. Chem., Int. Ed.* **2002**, *41*, 2821.
(26) Xie, L.; Liu, S.; Gao, C.; Cao, R.; Cao, J.; Sun, C.; Su, Z. *Inorg. Chem.* **2007**, *46*, 7782.
(27) Maniam, P.; Stock, N. *Inorg. Chem.* **2011**, *50*, 5085.
(28) Sun, C. Y.; Liu, S. X.; Liang, D. D.; Shao, K. Z.; Ren, Y. H.; Su, Z. M. *J. Am. Chem. Soc.* **2009**, *131*, 1883.
(29) Martens, J. A.; Jammaer, J.; Bajpe, S.; Aerts, A.; Lorgouilloux, Y.; Kirschhock, C. E. A. *Microporous Mesoporous Mater.* **2011**, *140*, 2.
(30) Bajpe, S. R.; Kirschhock, C. E. A.; Aerts, A.; Breynaert, E.; Absillis, G.; Parac-Vogt, T. N.; Giebeler, L.; Martens, J. A. *Chem.—Eur. J.* **2010**, *16*, 3926.
(31) Panda, T.; Pachfule, P.; Bannerjee, R. *Chem. Commun.* **2011**, *47*, 7674.
(32) Zimowska, M.; Michalik-Zym, A.; Poltowicz, J.; Bazarnik, M.; Bahranowski, K.; Serwicka, E. M. *Catal. Today* **2007**, *124*, 55.
(33) *SAINT-Plus*, version 6.22; Bruker Analytical X-Ray Systems, Inc.: Madison, WI, 2001.
(34) Sheldrick, G. M. *SHELX-97*; Bruker Analytical X-Ray Systems, Inc.: Madison, WI, 1997.
(35) Spek, A. L. *J. Appl. Crystallogr.* **2003**, *36*, 7.
(36) Eddaoudi, M.; Kim, J.; Wachter, J. B.; Chae, H. K.; O'Keeffe, M.; Yaghi, O. M. *J. Am. Chem. Soc.* **2001**, *123*, 4368.
(37) Moulton, B.; Lu, J.; Mondal, A.; Zaworotko, M. J. *Chem. Commun.* **2001**, 863.
(38) Abourahma, H.; Bodwell, G. J.; Lu, J. J.; Moulton, B.; Pottie, I. R.; Walsh, R. B.; Zaworotko, M. J. *Cryst. Growth Des.* **2003**, *3*, 513.
(39) Xue, D.-X.; Lin, Y.-Y.; Cheng, X.-N.; Chen, X.-M. *Cryst. Growth Des.* **2007**, *7*, 7.
(40) Rohlicek, J.; Husak, M. *J. Appl. Crystallogr.* **2007**, *40*, 600.
(41) Kim, J.; Chen, B.; Reineke, T. M.; Li, H.; Eddaoudi, M.; Moler, D. B.; O'Keeffe, M.; Yaghi, O. M. *J. Am. Chem. Soc.* **2001**, *123*, 8239.
(42) Allen, F. *Acta Crystallogr.* **2002**, *B58*, 380.
(43) Qu, F.; Li, N.-Q. *Electroanalysis* **1997**, *9*, 1348.
(44) *The Porphyrin Handbook*; Kadish, K. M., Smith, K. M., Guilard, R., Eds. Academic Press: San Diego, 2000−2003.
(45) Qiu, S.; Zhu, G. *Coord. Chem. Rev.* **2009**, *253*, 2891.
(46) He, J.; Zhang, Y.; Pan, Q.; Yu, J.; Ding, H.; Xu, R. *Microporous Mesoporous Mater.* **2006**, *90*, 145.
(47) Chen, J.; Ohba, M.; Kitagawa, S. *Chem. Lett.* **2006**, *35*, 526.
(48) Adam, W.; Griesbeck, A. G.; Klug, P.; Nestler, B.; Richter, M.; Wang, X. In *Selective Reactions of Metal Activated Molecules*; Werner, H., Griesbeck, A. G., Adam, W., Bringmann, G., Kiefer, W., Eds.; Vieweg: Braunschweig, Germany, 1992; p 149.
(49) Maurya, M. R.; Kumar, U.; Manikandan, P. *Dalton Trans.* **2006**, 3561.